

# Finger Grasp Kinematics Towards Exoskeleton Development

Lachlan R. McKenzie, Benjamin C. Fortune,  
Logan T. Chatfield, Chris G. Pretty

*Department of Mechanical Engineering, University of Canterbury,  
Christchurch, New Zealand*

**Abstract:** This paper investigates the relationships between index finger joint rotations to determine whether a one degree of freedom (DOF) exoskeleton could produce natural finger motions for a range of different users and grasping conditions.

Four healthy subjects each performed ten trials involving the grasp of two cylindrical objects with diameters of 66.5mm and 47mm. Finger trajectories for each trial were recorded using a motion capture system and were used to obtain joint rotational trajectories for the Metacarpophalangeal (MCP) Proximal-interphalangeal (PIP) and Distal-interphalangeal (DIP) joints.

Joint ranges of motion (ROM) were largest for all subjects when grasping the smaller diameter object. This effect was also seen where subjects with longer fingers tended to use a larger MCP ROM for the same object. Subject 2 was an exception to this, using the smallest MCP and PIP ROM of all subjects when grasping the large diameter object: this anomaly is thought to be caused by difference in palmar engagement with the object.

The profile of the MCP-PIP trajectories were similar when normalised to their range of motion, with a maximum y-axis error of 22%. This implies that the MCP-PIP relationship for a cylindrical grasp can be approximated by a general scalable polynomial. We conclude that through parabolic coupling between MCP and PIP joints, a one-DOF exoskeleton is capable of producing functional grasping movements. Through an adjustable coupling mechanism between MCP and PIP, it is also believed that an exoskeleton can be successfully adapted for differing object and finger sizes.

*Keywords:* Stroke Rehabilitation, Exoskeleton, Finger Kinematics, Grasp

## 1. INTRODUCTION

Globally, stroke is the second most prominent cause of death and is one of the leading causes of disability (World Stroke Organisation, 2017). Stroke patients typically suffer from hemiparesis, a condition that manifests as weakness of the contralesional side of the body. Such physical deficits, especially in the upper-extremities and hand, can prevent a patient from performing basic activities of daily living (ADL). Robotics and exoskeletons contain considerable potential for stroke rehabilitation, having the ability to provide therapy that is consistent, high intensity, and interactive.

The hand is a complex structure consisting of many degrees of freedom (DOF): this nature allows the hand to produce the broad spectrum of movements used in everyday life. Accounting for the full complexity of the hand, however, would give rise to convoluted and cumbersome exoskeleton designs. Therefore, hand exoskeleton designers often take steps to simplify the anatomical model. The most common finger model adopted in hand exoskeleton design is a four-DOF revolute chain (Sarakoglou et al., 2016), as seen in Fig 1. Adduction/abduction and flexion/extension of the Metacarpophalangeal joint (MCP)

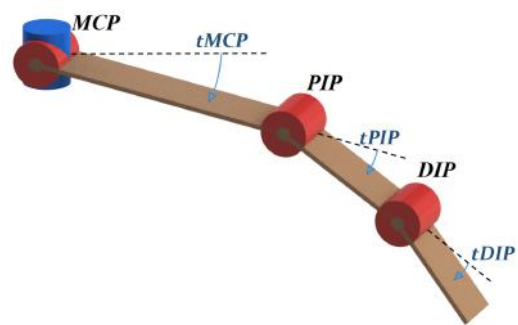


Fig. 1. Simplified finger model four-DOF revolute chain. MCP, PIP, and DIP are the Metacarpophalangeal, Proximal Interphalangeal, and Distal Interphalangeal joints, respectively. tMCP, tPIP, and tDIP, are the joint rotations for the MCP, PIP, and DIP joints, respectively

for the first two DOF. The final two DOF are covered by the flexion/extension of the Proximal Interphalangeal (PIP) and Distal-Interphalangeal (DIP) joints.

In current exoskeleton technologies, there is diversity in the support of finger joints and DOF. Some designers, such as Kawasaki et al. (2007) and Li et al. (2011) opt to obtain independent control of the finger joints through the use of one actuator per DOF: the resulting exoskeleton will be highly controllable and have a large reachable workspace. Kinematic designs of such exoskeletons are simplified, as the designer only needs to consider the reachable workspace of a human finger, so more design emphasis can be placed on aspects such joint torque and velocities. However, an actuator per DOF will cause portability issues due to added weight, size, and power requirements.

Alternatively, designers may choose to reduce the number of actuators to help alleviate issues of exoskeleton weight and size. There are a number of ways to reduce the number of system actuators, such as under-actuation, where the added mobility of elastic/passive elements allow less driving sources than DOF (Sarac et al., 2017). Under-actuation of a finger-exoskeleton can result in a simpler device without constraining the finger workspace. However, complete control of finger joint posture cannot be achieved (Chiri et al., 2012).

Reducing the exoskeleton DOF lessens the requirements for actuation. DOF reduction can be achieved by neglecting a finger phalanx (Taheri et al., 2014; Takagi et al., 2009), however, is more commonly accomplished through coupling of joint motions. By introducing DOF-coupling, the mechanism's range of motion is spatially constrained: consequently, the success of the design can be reliant on the assumptions that are applied in this process.

A number of stroke-rehabilitation exoskeletons possess only one DOF. This reflects findings that basic curling motion is the predominant finger movement incorporated into most activities of daily living (Taheri et al., 2014). Yang et al. (2016) further supports this notion, recommending that recovery of the hand's normal curling function should have priority over more complex movements.

### 1.1 Intra-finger Constraints

For a one-DOF exoskeleton to facilitate natural finger movements, the rotational couplings need to mimic that of a normal finger. Therefore, kinematic study of the finger gives valuable insight to an exoskeleton designer.

The strongest intra-finger constraint appears to be between the PIP and DIP joint rotations (tPIP, tDIP). Linear tPIP to tDIP coupling has been reported in a range of literature (Cobos et al., 2007; Rijpkema and Girard, 1991; Chen Chen et al., 2013), and has been applied in exoskeleton/prosthetic technologies (Lin et al., 2000; Liu and Zhang, 2007).

A coupling definition between the MCP joint rotation (tMCP) and distal joint rotations is less established. Kamper et al. (2003) investigated stereotypical fingertip trajectories over a range of grasps and found no characteristic relationship between the tMCP and tPIP. MCP to PIP joint rotations have also been investigated by Yang et al. (2016) and Jo et al. (2019) throughout finger flexion/extension movements. Yang et al. (2016) found tMCP and tPIP to be more coupled during finger extension, and found a fourth

order polynomial to describe the coupling. As noted by Jo et al. (2019), the finger's adaptation to an object's size and shape, as well as individuals grasping habits, can cause difficulty in finding a characteristic relationship between tMCP and tPIP. In neither investigation were the participants instructed to grasp an object.

The objective of this study is to further investigate the rotational coupling between MCP and PIP joints. We aim to study finger motion over a series of cylindrical grasp tasks to determine whether differing object diameter and differing finger length have an impact on the tMCP-tPIP relationship. This information will give insight as to whether a one-DOF exoskeleton could produce natural finger motion for a range of different users and grasping conditions, that closely resemble ADL.

## 2. METHODS

Four healthy subjects participated in a series of grasping trials. The subjects were three male and one female, aged  $24 \pm 1$ .

Subjects were seated at a table with two cylindrical objects placed in front of them. The objects, sauce and chilli, with diameters 66.5mm and 47mm, respectively, were orientated in an upright position, see Fig. 2. Throughout the trial, the subjects were instructed to reach and lightly grasp an object with their dominant hand. There were no specific instructions given on how to grasp the object, in an attempt to promote a natural grasping motion. Between grasping motions, the subject's hand rests in a comfortable posture on the table.



Fig. 2. Objects, sauce (left) and chilli (right), with diameters 47mm and 66mm respectively

Ten grasping trials per object were completed, with the order of grasping instructions randomised. Every five grasps, the subject was given thirty seconds of rest. After the completion of the grasping trials, subject's proximal-phalanx (PPh), inter-phalanx (IPh), and distal-phalanx (DPh) of the index finger were measured with digital calipers. The DPh length was set as the distance from DIP joint to fingertip.

The finger was tracked using a motion capture system with six cameras (Prime 13, Optitrack) that recorded position of reflective markers at 240 Hz. Twelve reflective markers were placed on the index finger of the subject's

dominant hand. Trajectory data was smoothed through Optitrack by a 4th order low-pass Butterworth filter with frequency cutoff of 6 Hz. Data analysis was performed using MATLAB (2018b).

The markers were placed on the finger such that the proximal phalanx, intermediate phalanx, distal phalanx, and hand-base form separate rigid bodies, see Fig 3. At the beginning of each recording session, the subject's finger was placed along the global x-axis and the rigid bodies calibrated to coincide with the global coordinate system, depicted in Figure 4. Joint angles for the MCP, PIP, and DIP could then be obtained through the relative position and orientation of the rigid bodies.

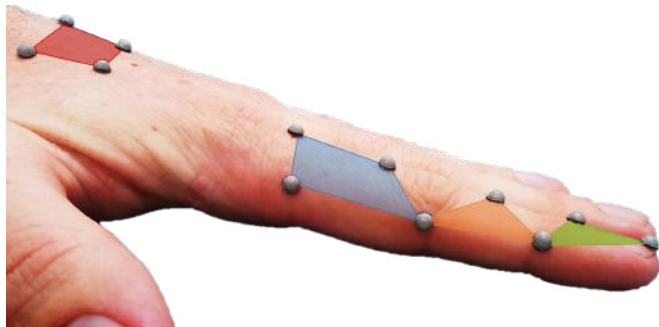


Fig. 3. Reflective Marker Placement on Hand. Rigid bodies for hand-base, proximal phalanx, intermediate phalanx, and distal phalanx are defined as indicated by the red, blue, orange, and yellow polygons, respectively.

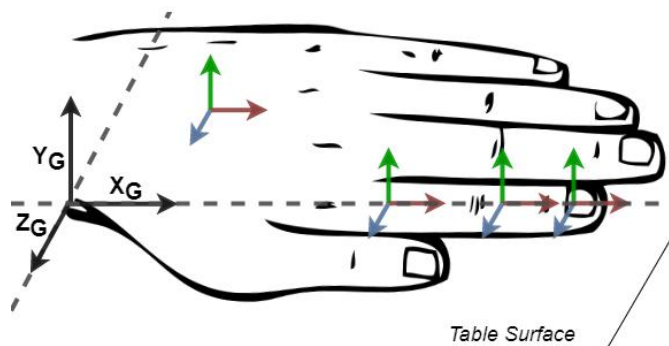


Fig. 4. Calibration of the hand local coordinate system (x - red, y - green, and z - blue) with the global camera coordinate system ( $X_G$ ,  $Y_G$ ,  $Z_G$ )

The trajectory of the MCP joint was used to define the active portion of each grasping trial. The midpoint of grasp was approximated as the mean of the maximum and minimum joint angles. The data were filtered through a 12.5 ms moving average and differentiated. The end of the grasp was identified by finding the first locus at which the  $\frac{\delta tMCP}{\delta t} < 3^\circ s^{-1}$ . The start of the grasp is determined in a similar manner, looking backwards from the midpoint.

For each subject, joint data was collated into sets for the chilli grasping task and sauce grasping task. The relationship between tMCP-tPIP and tPIP-tDIP for each task was observed. The PIP joint rotations were treated as the independent variable. The tMCP to tPIP relationship was

approximated as a second order polynomial, and tPIP to tDIP relationship approximated as linear. To provide ease of comparison, each subject's data-sets were translated so that the polynomial and linear approximations intercept each axis at the origin. This simplifies the approximation forms to

$$tMCP = \alpha tPIP^2 + \beta tPIP, \quad (1)$$

$$tDIP = \gamma tPIP. \quad (2)$$

### 3. RESULTS

Table 1 contains the measured finger-length for each subject, broken into PPh, IPh, and DPh segments.

Table 1. Subject's total finger, proximal-phalanx (PPh), inter-phalanx (IPh), and distal-phalanx (DPh) lengths, in millimeters.

Subject	Total Finger	PPh	IPh	DPh
1	91.3	43.5	25.5	22.3
2	90.7	43.4	25.3	22.0
3	103.5	48.7	28.0	26.8
4	82.3	39.3	23.0	20.0

Table 2 contains subject PPh, IPh, and DPh lengths, normalised to their total finger lengths.

Table 2. Subjects's normalised proximal-phalanx (nPPh), inter-phalanx (nIPh), and distal-phalanx (nDPh) lengths

Subject	nPPh	nIPh	nDPh
1	0.4765	0.2793	0.2442
2	0.4785	0.2789	0.2426
3	0.4705	0.2705	0.2589
4	0.4775	0.2795	0.2430

Figures 5 and 6 depict a subject's non-translated data collected over one set of grasping tasks, and the approximation fit to the data.

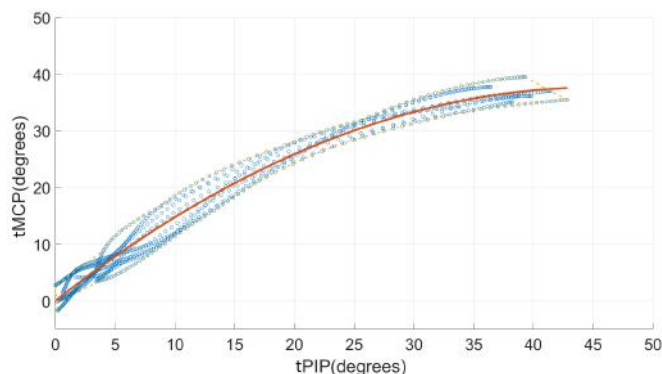


Fig. 5. Relationship between tMCP and tPIP joints of Subject 3 for the chilli grasping trials (blue) showing the quadratic fit (red).

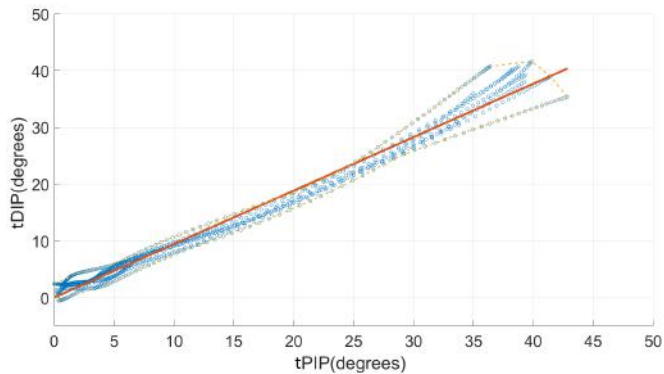


Fig. 6. Relationship between tPIP and tDIP of Subject 3 for the chilli grasping trials (blue) showing the linear fit (red).

Table 3 shows the tMCP-tPIP polynomial coefficients ( $\alpha$ ,  $\beta$ ) calculated for each subject over the chilli and sauce trials. Table 4, shows the calculated tPIP-tDIP coupling ratios ( $\gamma$ ). For each approximation, Pearson's correlation coefficient ( $R^2$ ) was computed to provide an estimate of the goodness of fit.

Table 3. Polynomial coefficients and corresponding Pearson's correlation coefficients.

Subject	Chilli			Sauce		
	$\alpha$	$\beta$	$R^2$	$\alpha$	$\beta$	$R^2$
1	-0.0160	1.2458	0.96	-0.0087	1.2200	0.98
2	-0.0155	0.9826	0.88	-0.0233	1.9566	0.97
3	-0.0182	1.6583	0.99	-0.0073	1.5177	0.99
4	-0.0072	0.7019	0.96	-0.0052	1.0089	0.97

Table 4. Linear regression coefficients and corresponding Pearson's correlation coefficients.

Subject	Chilli		Sauce	
	$\gamma$	$R^2$	$\gamma$	$R^2$
1	1.0402	0.78	1.0443	0.86
2	1.0604	0.87	0.8177	0.88
3	0.9423	0.81	1.0057	0.7115
4	0.9403	0.97	0.7469	0.87

The range of motion along with polynomial fit for subject's tPIP-tMCP data are depicted in Fig 7 and Fig 8 for ten chilli and ten sauce trials each, respectively. Envelopes are provided to indicate the extent of the data for each subject.

Table 5 shows the range of motion covered by tPIP and tMCP during chilli and sauce trials. The range of motion is determined from the characteristic polynomial fitted for each subject's collated data.

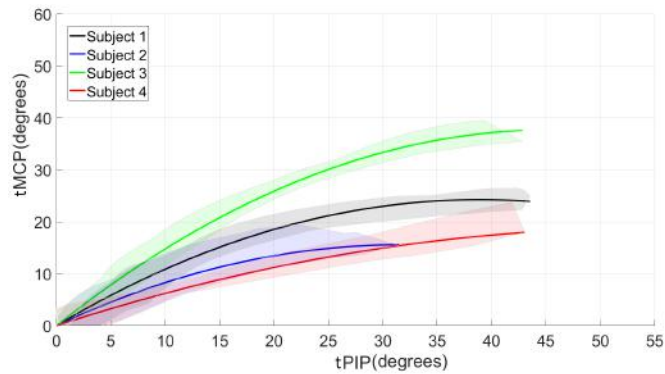


Fig. 7. Envelope of tPIP-tMCP motion and fitted characteristic polynomials for ten chilli grasping trials each subject.

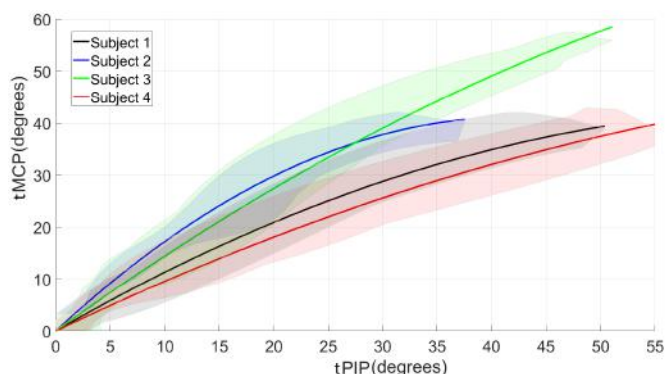


Fig. 8. Envelope of tPIP-tMCP motion and fitted characteristic polynomials for ten sauce grasping trials each subject.

Table 5. tMCP and tPIP range of motion for sauce and chilli trials.

Subject	Chilli		Sauce	
	$\theta_{MCP}$	$\theta_{PIP}$	$\theta_{MCP}$	$\theta_{PIP}$
1	23.9	43.5	39.4	50.4
2	15.6	31.5	40.7	37.6
3	37.6	42.8	58.5	51.1
4	17.9	43.0	40.4	56.5

Fig 9 shows the motion profiles for each subject over each trial, normalised with respect to range of motion. The maximum range in MCP for a given PIP is 22%.

#### 4. DISCUSSION

Linear regression characterised tPIP-tDIP well using first order poles, with the lowest  $R^2$  coefficient being 0.71. During the chilli-grasping trials, a coupling ratio near one-to-one was identified for all subjects. This ratio is higher than the ratios identified by others Kamper et al. (2003); Cobos et al. (2007). Over the sauce-grasping trials, tPIP-tDIP coupling remained relatively consistent for Subjects 1 and 3, and dropped to 0.82 and 0.75 for Subjects 2 and 4. Over the range of circular grasps performed in this study, the relationship between PIP and MCP joint rotations was well characterised by a second-order polynomial, with the lowest  $R^2$  of 0.88.

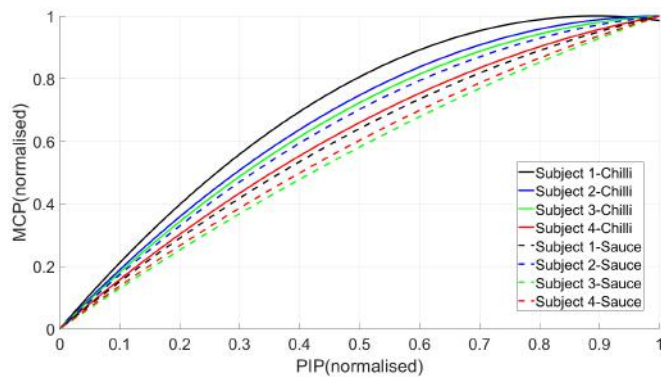


Fig. 9. Subject trajectories normalised over range of motion.

Larger ranges of motion for MCP and PIP joint angles were utilised throughout the sauce grasping trials. This effect was identified in joint trajectories for all subjects. The relative diameters of the object largely contribute to this pattern. The chilli jar has diameter of 66.5 millimetres whilst the sauce bottle's diameter is 47 millimetres. The finger phalanx will naturally need to flex more to properly wrap around the sauce bottle's smaller circumference. Another identified trend is the larger increase in MCP flexion with respect to PIP flexion. The mean increase in MCP flexion between chilli and sauce objects was  $21^\circ$  across all subjects whilst the mean increase in PIP flexion was  $8.7^\circ$ : this suggests that the subject's predominately used their MCP joint to adapt to change in grasp diameter.

Difference in finger-length was also seen to impact tPIP-tMCP flexion range throughout the grasping trials. Subjects with longer fingers tended to rotate finger joints throughout a larger range of motion than those with smaller fingers. This is principally due to the relative size of the finger with respect to object circumference. Difference between grasp trajectories for Subject 1 and Subject 4 in Fig 7 and Fig 8 depict the effect of different finger lengths. Subject 3's index finger is 21.1mm longer than Subject 4's index: flexion of Subject 3's MCP joint exceeds Subject 4's MCP by  $19.7^\circ$  and  $18.1^\circ$  for chilli and sauce grasps, respectively. Once again, difference in MCP range of motion dominates the difference in motion profiles.

The motion profiles recorded for Subject 2 show abnormalities with respect to the other three Subjects. Seen in Fig 7, both tPIP and tMCP for Subject 2 exhibit the smallest range of motion, despite Subject 2's finger-length being 8.4 millimetres larger than Subject 4, and only 0.6 millimetres shorter than Subject one. Additionally, the normalised phalanx lengths for Subject 2 are similar to the other subjects. The motion of Subject 2 for the chilli grasping sequence therefore violates our earlier assumption that a larger finger results in greater phalanx flexion. It is suspected that Subject 2 did not fully engage the palm during the grasping motion, causing the chilli jar to be grasped more distally by the fingers. Subject 2's individuality in grasping habits also features throughout the sauce trials: at the start of the motion Subject 2 exhibits the steepest coupling relationship between tMCP and tPIP. Additionally, Subject 2's tPIP range of motion is the smallest of all subjects during the sauce trials.

The trajectories for all subjects and objects, when normalised by their range of motion, exhibit a similar motion profile (the maximum range in MCP for a given PIP is 22%). This implies that tMCP-tPIP relationship for the index finger for a cylindrical grasp can be approximately characterised by a general polynomial that is scalable to a desired range of motion. Naturally, a general polynomial cannot capture or mimic the idiosyncrasies of every individuals grasping habits (as humans are horribly variable (Dickson et al., 2014)). However, through the trials conducted in this study it has become apparent that, for the same movement task, there are a range of finger trajectories that can be employed. This effect is depicted by the envelope of trajectories recorded for each subject and each task. Furthermore, the motion profiles recorded for Subject 2 indicate that finger-joint couplings can be easily altered through slightly different grasping strategies. So, the kinematics don't need to perfectly reflect the natural grasp.

Towards exoskeleton design-based outcomes, we believe that functional grasping movements can be promoted through the parabolic coupling of MCP and PIP joint rotations. Through design of an adjustable coupling mechanism, the exoskeleton design will be able to adapt to a change of object diameters and a range of finger sizes.

#### ACKNOWLEDGEMENTS

Funding from a HOPE-Selwyn Foundation Scholarship in Ageing Research is gratefully acknowledged.

#### REFERENCES

- Chen Chen, F., Appendino, S., Battezzato, A., Favetto, A., Mousavi, M., Pescarmona, F., 2013. Constraint study for a hand exoskeleton: Human hand kinematics and dynamics. *Journal of Robotics* 2013.
- Chiri, A., Vitiello, N., Member, S., Giovacchini, F., Roccella, S., Vecchi, F., Carrozza, M. C., Member, A., 2012. Mechatronic Design and Characterization of the Index Finger Module of a Hand Exoskeleton for Post-Stroke Rehabilitation 17 (5), 884–894.
- Cobos, S., Ferre, M., Sánchez-Urán, M., Ortego, J., 2007. Constraints for Realistic Hand Manipulation. *Proc. Presence 2007*, 369–370.
- Dickson, J. L., Gunn, C. A., Chase, J. G., 2014. Humans are Horribly Variable. *International Journal of Clinical & Medical Imaging* 1 (2), 1000142.
- Jo, I., Park, Y., Lee, J., Bae, J., 2019. A portable and spring-guided hand exoskeleton for exercising flexion/extension of the fingers.
- Kamper, D. G., Cruz, E. G., Siegel, M. P., 2003. Stereotypical fingertip trajectories during grasp. *Journal of neurophysiology* 90 (6), 3702–3710.
- Kawasaki, H., Ito, S., Ishigure, Y., 2007. Development of a Hand Motion Assist Robot for Rehabilitation Therapy by Patient Self-Motion Control 00 (c), 234–240.
- Li, J., Zheng, R., Zhang, Y., Yao, J., 2011. iHandRehab: An interactive hand exoskeleton for active and passive rehabilitation. *IEEE International Conference on Rehabilitation Robotics* (50975009).
- Lin, J., Wu, Y., Huang, T. S., 2000. Modeling the constraints of human hand motion. *Proceedings - Workshop on Human Motion, HUMO 2000*, 121–126.

- Liu, J. L. J., Zhang, Y. Z. Y., 2007. Mapping human hand motion to dexterous robotic hand. 2007 IEEE International Conference on Robotics and Biomimetics (ROBIO), 829–834.
- Rijpkema, H., Girard, M., 1991. Computer animation of knowledge-based human grasping. *ACM SIGGRAPH Computer Graphics* 25 (4), 339–348.
- Sarac, M., Solazzi, M., Sotgiu, E., Bergamasco, M., Frisoli, A., 2017. Design and kinematic optimization of a novel underactuated robotic hand exoskeleton. *Meccanica* 52 (3), 749–761.
- Sarakoglou, I., Brygo, A., Mazzanti, D., Hernandez, N. G., Caldwell, D. G., Tsagarakis, N. G., 2016. Hexotrac: A highly under-actuated hand Exoskeleton for finger tracking and force feedback. *IEEE International Conference on Intelligent Robots and Systems 2016-Novem*, 1033–1040.
- Taheri, H., Rowe, J. B., Gardner, D., Chan, V., Gray, K., Bower, C., Reinkensmeyer, D. J., Wolbrecht, E. T., 2014. Design and preliminary evaluation of the FINGER rehabilitation robot: controlling challenge and quantifying finger individuation during musical computer game play. *Journal of NeuroEngineering and Rehabilitation* 11 (1), 10.
- Takagi, M., Iwata, K., Takahashi, Y., Yamamoto, S. I., Koyama, H., Komeda, T., 2009. Development of a grip aid system using air cylinders. *Proceedings - IEEE International Conference on Robotics and Automation*, 2312–2317.
- World Stroke Organisation, S., 2017. Face the Facts: Stroke is Treatable.
- Yang, J., Xie, H., Shi, J., 2016. A novel motion-coupling design for a jointless tendon-driven finger exoskeleton for rehabilitation. *Mechanism and Machine Theory* 99, 83–102.